

Chemical Evolution of Groundwater in the Dindéfello Plain Area in South-Eastern Senegal

Seybatou Diop¹, Moshood N. Tijani²

¹Institute of Earth Sciences, Faculty of Sciences and Techniques, Cheikh Anta Diop University of Dakar, Dakar, Senegal

²Department of Geology, University of Ibadan, Ibadan, Nigeria
Email: seybdiop@yahoo.fr, tmoshood@yahoo.com

Received 19 November 2014; revised 10 December 2014; accepted 26 December 2014

Copyright © 2014 by authors and Scientific Research Publishing Inc.
This work is licensed under the Creative Commons Attribution International License (CC BY).
<http://creativecommons.org/licenses/by/4.0/>



Open Access

Abstract

This study was to clarify the main mechanisms of shallow groundwater mineralization in the Dindéfello Plain Area. Water composition data obtained in this study were subjected to aqueous speciation calculations together with data plotting on key diagrams so as to create work assumptions. Hypothesized reaction models of the processes of chemical weathering of carbonates and silicate minerals under the carbon dioxide regime were proposed and tested by selecting two water sample analyses interpreted as “starting” and “ending” water composition along a hydrologic flow line, and then running the PHREEQC (version 2) batch modeling procedure, to simulate chemical balances and compositional variations of groundwater within the geochemical system. For the flow path data discussed here, there was close agreement between the model results and the observed hydrochemistry, and so the proposed geochemical evolution model was deemed reliable.

Keywords

Senegal, Dindéfello, Groundwater, Mineralization, Springwater, Geochemical Modeling

1. Introduction

The composition of groundwater is an important source of hydrogeochemical information about earth surface weathering processes [1]. Hence, knowledge of the solute constituents could aid in reconstructing the major chemical reactions contributing to groundwater mineralization ([2]-[8]). The purpose of the exercise was to demonstrate a proposed hypothesis of Diop *et al.* [9], that the main control on groundwater mineralization in the

near surface aquifers of the DPA hydrologic system (hereinafter referred to as DPA-HS) is the pH-driven process of mineral breakdown (mainly carbonates and silicates), under the carbon dioxide regime. This paper is based on the interpretation of water composition data presented by these authors, and it follows a two-step procedure.

In the first instance, key diagrams pertinent for inferring the hydrogeochemical evolution of groundwater in the DPA-HS are presented, and then the batch modeling procedure of PHREEQC computer program (version 2, [10]) to reconstruct the hypothesized reaction models is run. In essence, this simulated the specific case that recharge spring water infiltrating into the ground interacts along its flow paths with calcite, dolomite and albite minerals under “open-system conditions” [4] to account for the observed chemical composition of groundwater downstream.

2. Location and Hydrogeology

The study area is located on the Senegal-Guinea Republic border, between longitude 12°20'W - 12°25'W and latitude 12°20'N - 12°25'N, within a region referred to here as the “Dindéfello Plain Area”—DPA.

The DPA is a poorly documented depression bounded to the south by a range of hills rising to over 400 m above the surrounding terrain, with maximum elevations approximately 450 m above MSL (Figure 1). Fracture and contact springs are found at the margins of the top of the plateau and its foothills. The regional structures are components of the *Fouta Djallon Mountains* chain (Guinea Republic), which is emplaced on the southern prolongation of the *Mauritanides* fold belt ([11] [12]). Organically, the *Mauritanides* belt flanks the 2×10^9

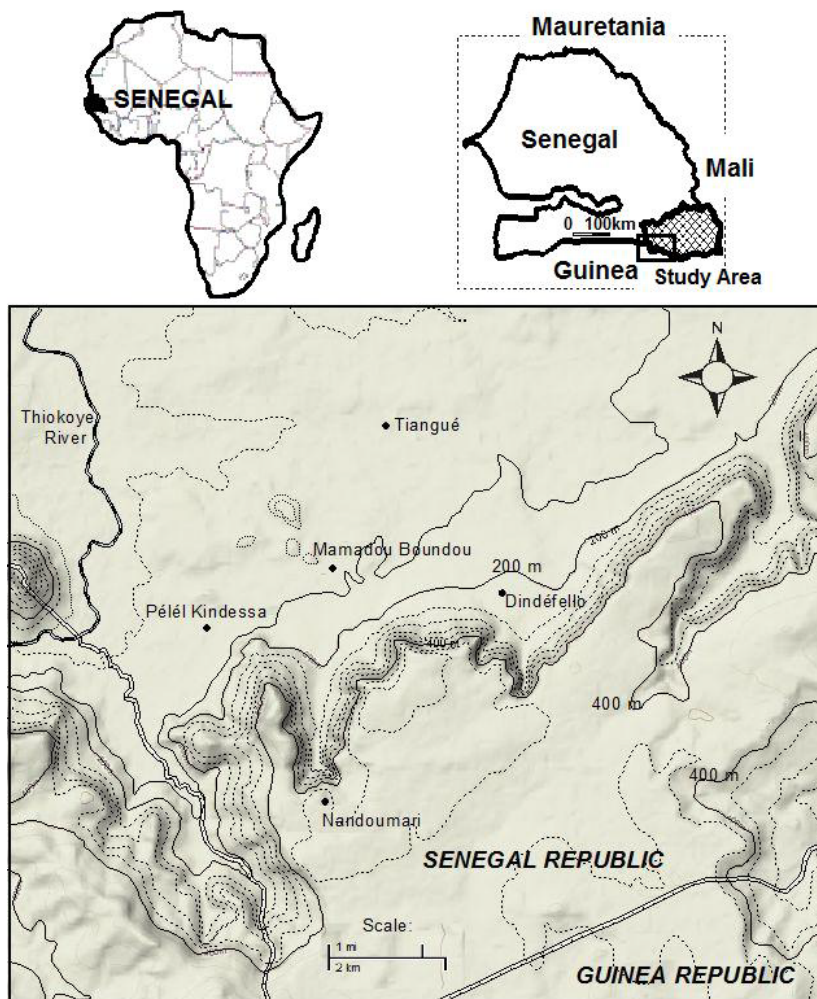


Figure 1. Location map of the study area within south-eastern Senegal.

years old West African craton to the west ([13] [14]). Rocks underlying the DPA, or outcropping, are mainly young basement rocks of the Ségou-group ([15]-[18]) which contain mineralogical groupings (carbonaceous limestones and dolostones and feldspatic sandstones assemblages) that are source of major ions in the groundwater of the study area.

The groundwater system underlying the DPA comprises the low-permeability regolith zone (upper aquifer unit with the water table mostly 10 - 30 m below ground surface), and the more productive adjacent zone reservoir of bedrock disintegration and leaching (lower aquifer unit). There is interaction between this system and the topography-driven spring water system that flows out of the uplands and avalanches down into the plain area.

Recharge to the subterranean drainage system occurs on a yearly basis, as spring discharges cascade down onto the valley floors and drain into pathways incised by the river system, and remain in the channel over a long distance. However, the low permeability character of the superficial regolith reduces the effectiveness of direct rainwater infiltration. Thus, groundwater is recharged locally and essentially by runoff in the alluvium of rivers and their tributaries, which have eroded their ways into the plain floor. Spring water percolating downward through the alluvium of river channels reaches the groundwater table, thereby forming a major source of groundwater recharge. The hydrodynamic regime of the hydrologic system is topography-driven and the land surface can be used to infer groundwater flow patterns, assuming that the water table is a subdued replica of the surface topography.

In the study area domestic water supply is typically obtained from shallow hand-dug wells bored in the regolith zone reservoir, down to depths of 20 - 30 m below ground surface. The water level in these wells can rise 10 m during the rainy season and then can fall almost rapidly. However, a more permanent supply is reached by motor-driven wells that penetrate the deeper seated fractured zone reservoir. During the rainy season from May to October, this region receives about 1200 mm rainfall, of which nearly 20% may result as net rain [19]. During the dry season, surface water sources are very limited, and the depth of groundwater is relatively great (often >25 - 30 m). To meet their water needs in this period, people most frequently collect water from springs and pondlets dug on stream beds.

3. Materials and Methods

Traditionally, the geochemistry of groundwater can be used to reconstruct the controlling processes of mineral dissolution. Theories on the origin of groundwater mineralization generally agree that when water comes into contact with minerals, chemical weathering and dissolution of the minerals begins and continues until equilibrium concentration is attained in the water, or until all minerals are consumed [4]. Thus, depending on the environment, chemical and mineralogical characteristics of the rocks which groundwater has come into contact with during its flow history, its chemistry may be altered to reflect the host rocks. Because of this, one inclination might be to use the equilibrium concept as a means of interpreting chemical data. So, if water samples need to be checked as to how far the hypothetical reactions have proceeded to give their hydrochemistry, their SIs with respect to these minerals should be calculated. For a given water sample, its SI with respect to any candidate source or sink mineral can be computed, based on the ionic product for the aqueous phase and its equilibrium constant at the considered temperature.

It is not intended here to describe the theoretical background (for more details, see [4], [20] or [21]), but, instead, to note that the saturation state for a particular mineral (considered as possible source or sink of ions to aqueous solution), or other participating substance is expressed as saturation index (SI), [20]:

$$SI = \log I_{aq} / K_{(T)}$$

where:

I_{ap} : ionic activity product

K_T : mineral equilibrium constant at the specified temperature.

- For $SI > +0.1$, the specific mineral is supersaturated, and precipitation is possible;
- For $-0.1 < SI < +0.1$, the specific mineral is saturated and precipitation or dissolution possible; and
- For $SI < -0.1$, the specific mineral is undersaturated, and dissolution possible.

The approach taken was to first carry out exploratory investigations for mineral-water relationships from the analyzed data so as to create work assumptions, and then use the computer program PHREEQC (<http://water.usgs.gov/software/>) to check these assumptions.

The data used for this study (**Table 1**) were essentially the major elements' chemistry of water samples from springs, water supply pondlets dug by villagers on stream beds and village hand-dug wells. **Figure 2** conveys the areal distribution of the various samples. Supplementary data included the chemical composition of rainfall [22] which was found to be available and so allowed comparison with spring water (**Table 1**), as well as compiling qualitative data about the nature of the physical environment. This enabled approximating groundwater flow patterns to be drawn (by assuming that the water table is controlled by the surface topography), thus providing a comprehensive inventory of potential reactants for the proposed geochemical model evolution.

4. Results and Discussions

4.1. Analysis of Trend

The data employed in this study is as presented in **Table 1**. The waters have acidity at near neutral pH ($4.65 \leq \text{pH} \leq 6.93$), and total mineralization (TDS) ranged from 20 to 570 mg/L. The five elements HCO_3^- , SiO_2 , Ca^{2+} , Mg^{2+} and Na^+ , in order of decreasing abundance, make up the bulk of mineralization. These elements represent over 80% - 90% of the TDS. In a general way, subsurface groundwater (*i.e.* water samples from hand-dug wells) has much higher mineralization than spring water, which shows near-local rainwater characteristics. The consistently lower mineralization of spring water indicated rapid drainage of meteoric waters through the high permeability pathways provided by rock fractures, joints, bedding planes and faults in the highlands. This rapid flow results in shorter residence time and less mineral-water interaction in the host rocks. However, anomalously high TDS of some springs (Pr3 and 14) and pondlets (Pr4 and 5) revealed the influence of marshy conditions prevailing at these locations where water may be acidic from CO_2 production (from organic matter decay) leading to increased solubility. In contrast, groundwater travelling in the plain aquifers generally had increasing levels of dissolved solids with distance down gradient as a result of chemically evolved recharge waters from longer residence time. Consequently, a model of hydrochemical evolution must explain the increase in dissolved solids, and hence the evolution of recharge spring water (or meteoric water), as it avalanches down onto the valley floor and infiltrates into the ground to become subsurface groundwater.

Moreover, **Table 1** shows that the higher its mineralization grade (column 3), the more groundwater is approaching equilibrium/saturation with respect to calcite, dolomite and aqueous silica (column 13 to 20). It seems reasonable, therefore, to suggest these three minerals as possible sources of dissolved constituents for groundwater. **Figure 2** and **Figure 3** represent key diagrams as regards the geochemical conditions giving rise to groundwater chemistry.

Figure 3 indicates the major compositional water types observed by plotting the samples in a Piper diagram whereby the circle radius is a scale for TDS. The chemical composition of most spring samples shows a minor nitrate and chloride impairment (possibly due to human impact), that causes them to vaguely shift along the $(\text{SO}_4 + \text{Cl} + \text{NO}_3)$ -axis of the lozenge and slightly obfuscate the evolutionary path for cations. The grouping shows:

1) Waters whose solutes are dominated by $\text{Ca}^{2+} + (\text{Mg}^{2+}) - \text{HCO}_3^-$; These are waters in which calcium and magnesium amount 50% or more of the cation budget, and bicarbonate to more than 50% of the anions. They are typical of recharge water into carbonate hosted lithology, *viz.* a geological environment containing calcite and dolomite whereby the characteristically high $\text{Ca}^{2+} + (\text{Mg}^{2+}) - \text{HCO}_3^-$ levels suggest the geochemical implication of gas P_{CO_2} as a controlling factor.

2) Waters that are relatively enriched in alkali ions, comprising two cases of sodium bicarbonate end-member type, $\text{Na}^+ + (\text{K}^+) - \text{HCO}_3^-$; These are waters in which milliequivalents of $[\text{Na}^+ + (\text{K}^+)]$ and HCO_3^- contribute each more than 50% of the ion budget. They are distributed along the $(\text{Na} + \text{K})$ -axis of the Piper diagram in **Figure 3**, a distribution pattern that suggests chemically evolved type (1) waters through contemporaneous interaction with silicate rocks.

Figure 4 shows in this respect that the water composition, expressed in terms of SiO_2 and Na^+/H^+ , plots towards the boundary between kaolinite-Na-montmorillonite for spring waters, as compared to groundwater that characteristically evolves to the albite boundary as mineralization proceeds. Presumably albite dissolves incongruently to produce dissolved SiO_2 and Na in spring waters in the early stage of mineralization, and both kaolinite and Na-montmorillonite as secondary minerals by-products. The kaolinitic and Na-montmorillonitic by-products may dissolve subsequently as groundwater mineralization progresses. Several authors ([1] [3] [7]) have observed this behavior pattern in igneous terrains where most groundwater-derived surface waters, such as

Table 1. Water sample chemistry.

Water source	Label	Sum of ions	pH	HCO ₃ ⁻	Cl ⁻	SO ₄ ²⁻	Ca ²⁺	Mg ²⁺	K ⁺	Na ⁺	SiO ₂	SI Aragonite	SI Calcite	P _{CO₂} (g)	Dolomite	Gypsum	Anhydrite	SiO ₂ (a)	
Spring	Pr1	35	5.89	10.37	0.98	1.27	1.92	0.51	0.43	0.28	16.77	-4.23	-4.09	-1.85	-8.41	-4.69	-4.91	-0.84	
Spring	Pr2	37	5.91	11.59	1.3	1.93	1.8	0.7	0.61	0.38	15.98	-4.2	-4.05	-1.82	-8.17	-4.54	-4.76	-0.86	
Spring	Pr3	315	6.85	186.71	7.5	0.4	25.07	14.61	1.78	16.95	59.75	-1.03	-0.89	-1.58	-1.66	-4.32	-4.54	-0.29	
Pondlet	Pr4	492	6.93	325.22	0.54	2.03	84.7	10.36	1.52	8.05	57.2	-0.24	-0.09	-1.43	-0.75	-3.2	-3.42	-0.31	
Pondlet	Pr5	567	6.84	381.36	1.76	5.6	79.9	21.08	1.46	16.42	56.8	-0.3	-0.16	-1.28	-0.54	-2.82	-3.04	-0.31	
Spring	Pr6	63	4.65	25.61	1.32	0.09	2.46	0.81	1.16	1.16	13.36	-4.97	-4.83	-0.2	-9.79	-5.77	-5.99	-0.94	
Spring	Pr7	28	6.44	9.15	0.83	0.13	0.86	0.41	0.59	0.86	13.83	-4.08	-3.94	-2.45	-7.85	-6.02	-6.24	-0.93	
Spring	Pr8	23	5.16	6.1	0.35	0.04	0.57	0.25	0.45	0.32	12.79	-5.68	-5.54	-1.32	-11.08	-6.7	-6.92	-0.96	
Well	Pr9	519	6.44	290.44	8.21	6.71	103.7	9.95	0.82	9.87	58.31	-0.7	-0.55	-0.99	-1.78	-2.62	-2.84	-0.3	
Well	Pr10	269	6.35	103.73	0.29	0.35	17.18	2.83	2.78	13.38	126.91	-1.9	-1.76	-1.32	-3.95	-4.45	-4.67	0.04	
Well	Pr11	127	6.49	36.61	0.19	0.04	3.28	0.66	1.99	6.02	76.55	-2.88	-2.74	-1.91	-5.82	-6	-6.22	-0.18	
Spring	Pr12	32	6.43	10.98	1.45	0.8	1.05	0.63	0.63	1.13	13.84	-3.93	-3.79	-2.37	-7.45	-5.15	-5.37	-0.93	
Well	Pr13	238	6.57	74.44	4.43	0.67	10.04	1.23	3.42	15.82	123.08	-2.05	-1.9	-1.69	-4.37	-4.36	-4.58	0.02	
Spring	Pr14	416	6.68	233.7	0.54	2.4	39	21.43	1.49	4.5	111.32	-0.93	-0.79	-1.32	-1.49	-3.4	-3.62	-0.02	
Well	Pr15	497	6.53	291.66	3.3	3.15	81.24	13.47	0.9	9.51	87.12	-0.7	-0.56	-1.08	-1.54	-3.02	-3.24	-0.13	
Rainwater*		15.59	6.35	8.54	1.60	0.59	2.80	0.17	0.49	0.64	0.63								

All concentrations are in mg/l; *Mean chemical composition of rainfalls recorded at Kédougou weather station in the months of July and August 1981 [22]. Note the near saturation of some samples with respect to calcite, dolomite, CO₂ and SiO₂.

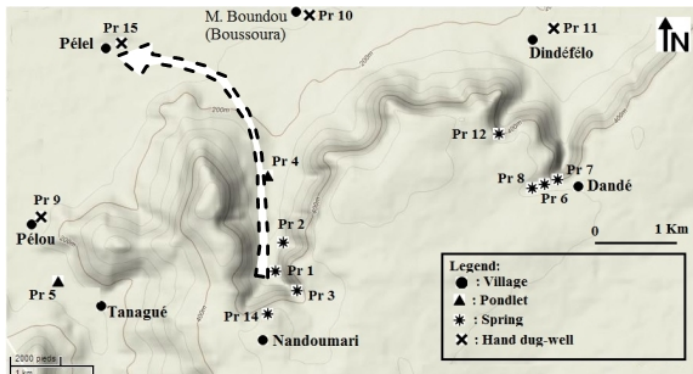


Figure 2. Location of the sampling sites within the DPA physiographic region. Note: The arrow indicates the simulated reaction flow path. Refer to **Figure 1** for the location of Pr13 (Tiangué Village).

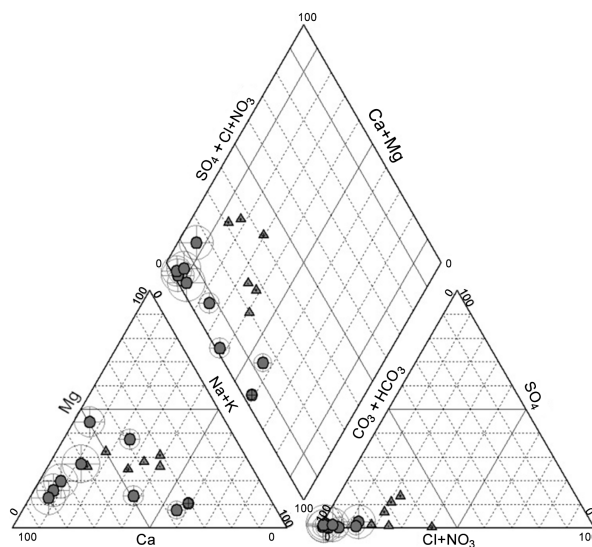


Figure 3. Piper diagram for the various water samples from the DPA-HS, with TDS as circles. Note: Triangles are springs water samples and circles represent groundwater samples.

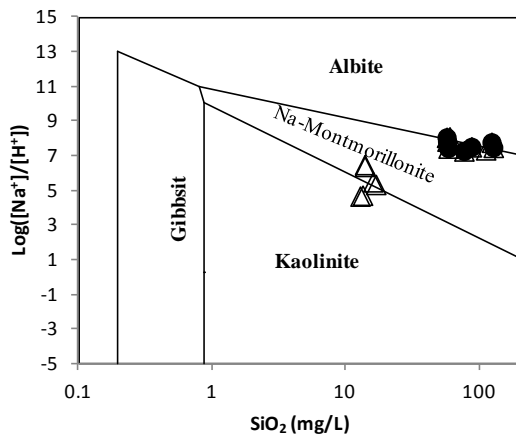


Figure 4. Stability diagram for gibbsite, kaolinite, montmorillonite and albite at 25°C. Note: Triangles are samples from springs, and circles represent samples from groundwater.

springs and baseflow, plot in the kaolinite fields of stability of this diagram type.

In **Figure 5** the water chemistry expressed in terms of pH and HCO_3^- is compared to the simple open-system dissolution model of [4] describing the evolution pattern of groundwater in contact with calcite at 15°C and under various partial pressures. It is obvious in this figure that all water samples plot above the atmospheric CO_2 partial pressure (P_{CO_2}) level of $10^{-3.5}$ bar; viz. within P_{CO_2} levels in ranges 10^{-1} - 10^{-3} bar which are at least 30-times the atmospheric level. This clearly means that water infiltrating through the aquifer soil zones become charged with CO_2 gas that normally makes water acidic and prone to weathering. Indeed, CO_2 normally reacts with water to form carbonic acid (H_2CO_3), which initiates geochemical reactions in groundwater.

It is obvious in **Figure 5** that spring waters occur with the lowest values of pH and HCO_3^- , while groundwater samples plot on a position near the calcite saturation line, thereby evolving within P_{CO_2} paths lines in the range roughly from 10^{-1} to 10^{-2} bar. Furthermore, the comparison in **Figure 5** also shows a regular increase in HCO_3^- with increasing pH (in the range 6 - 7) of groundwater where the higher its CO_2 partial pressure, the more groundwater is nearing equilibrium with respect to calcite. It is very likely that the hydrologic field situation for the dissolution of calcite to proceed roughly follows the evolution pattern described by the arrow. This trend has been interpreted to mean the conventional view point that more calcite dissolution leads to higher H^+ consumption and, therefore, to higher pH and HCO_3^- values, all according to the reaction:



As the dissolution reaction for calcite proceeds, consumption of H^+ (equivalent to a pH rise) normally causes the concentration of H_2CO_3 to decline however (according to: $\text{H}_2\text{CO}_3 \rightleftharpoons \text{H}^+ + \text{HCO}_3^-$) by fairly uniform CO_2 partial pressure within the range 10^{-1} - 10^{-2} bar. This implies that replenishment of the CO_2 stock (a CO_2 refill process from outside the system) must occur simultaneous as dissolved CO_2 is destroyed progressively on dissolution of calcite. Presumably, spring water regularly seeping into the ground as recharge water is an important source of CO_2 for groundwater. However, reaction types that tend to prevent a partial pressure drop within the system may include the conversion of calcite to wollastonite: $\text{CaCO}_3 + \text{SiO}_2 \rightleftharpoons \text{CaSiO}_3 + \text{CO}_2$ [23] and this factor is not included in this discussion. It is worth noting from the development above that HCO_3^- is from two different sources: 1) ionization of H_2CO_3 ($\text{H}_2\text{CO}_3 \rightleftharpoons \text{H}^+ + \text{HCO}_3^-$), and 2) reaction of H^+ with calcite ($\text{CaCO}_3 + \text{H}^+ \rightleftharpoons \text{Ca}^{2+} + \text{HCO}_3^-$), which probably explains its predominance in groundwater.

Additional sources of solute constituents in groundwater may include the weathering of other silicate compounds known to be present in the soil zone (e.g., potassium feldspar- KAlSi_3O_8) which is much less reactive than sodium feldspar— $\text{NaAlSi}_3\text{O}_8$ [2]. Also, aluminosilicate/clays minerals, as well as the dissolution of gypsum and cationic exchange, could be sources of solute in groundwater. Representing these reactions ([4] [5]) as in **Table 2** supports the contention that these are, perhaps, the more likely reactions to consider in explaining the major-ion chemical evolution of groundwater in the DPA. These reactions fairly illustrate how H^+ ions might be

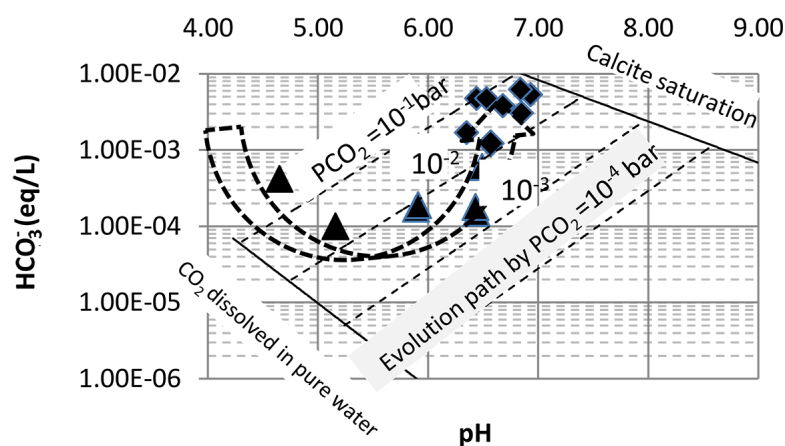
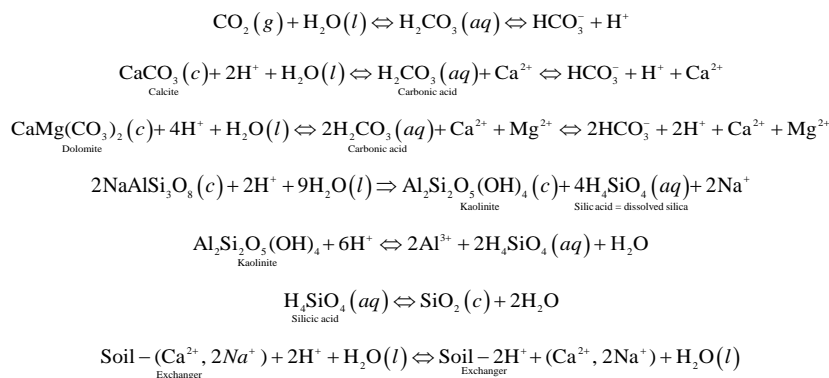


Figure 5. Plot of HCO_3^- as a function of pH according to the open-system dissolution model of Freeze and Cherry [4]. Note: Triangles are springs water samples and rectangles represent groundwater samples: The waters approach calcite saturation as dissolved HCO_3^- and H^+ increase.

Table 2. Set of possible chemical reactions which may control the hydrochemistry in aquifers of the DPA.

produced and consumed upon dissolution of the hypothesized minerals to result in the observed major ions' chemistry of groundwater.

4.2. Flow Path Modeling

The present research strongly suggests the CO₂-driven process of mineral weathering as being the most likely mechanism in controlling the hydrochemical evolution in the DPA. This is in keeping with the established views ([23] [24]) that CO₂-charged recharge waters from rain percolating into subsurface soils naturally dissolve mineral materials during their underground movement. The mechanisms occur either by equilibrium with soil zone CO₂ reservoir (or so-called “open system” conditions) or isolated from this reservoir (“closed system” conditions).

In the following assessment, the computer program PHREEQC (version 2; [10]) was used to investigate the control of hypothesized reactions on the water chemistry. This involved modelling the specific case where spring waters that are chemically identical to rain waters infiltrating at foothills (around sampling site Pr1), interact along their flow paths with the said minerals (viz. calcite, dolomite, albite and gibbsite) under “open-system” conditions to produce the major ion composition of groundwater sampled from a hand-dug well at site Pr15 (Pelel village), at about 3.5 km downstream of Pr1; (refer to **Figure 2** for the considered flow direction). This means that PHREEQC calculates speciation and moles of specified minerals and gas phases that would react with water sample Pr1 (initial solution) to produce an aqueous solution (final solution) whose mineral phases' SIs with respect to the considered match those for water sample Pr15.

The steps for the model implementation (see **Appendix**) are: 1) Definition of the numerical entities for running the model; 2) Input of the required information; and 3) Execute the simulation.

Once the calculations have been fulfilled to target saturation constraints (as defined by the modelling procedure under the heading “EQUILIBRIUM PHASES 1”; see Box 1 of List 1 in the **Appendix**), PHREEQC displays the output results.

The output file is lengthy and contains a wealth of information that is not presented here for the sake of brevity. For more details, see List 1 (**Appendix**), where the focal outcome is given in Box 3, under the subheadings “Phase assemblage” and “Solution composition”. Moreover, the chemical analysis of Pr15 was also included in the model for comparison with results of PHREEQC speciation for the output solution (see Box 4.2 of List 1 in the **Appendix**). As can be viewed from the comparison therein, the model reproduces the observed water chemistry reasonable well.

Table 3 is a shortcut for this comparison. It should be noted that the ionic increase from sample Pr1 to sample Pr15 was modelled (see column 2 of the table) as a down-gradient chemical change in the aquifer due to a greater magnitude of water-mineral-interaction along flow path; essentially carbonate and silicate minerals. Clearly, the model results (column 2) are in good agreement with the chemistry of the groundwater collected at site Pr15 (column 3). An illustration of the good quality of the prediction is given in **Figure 6** which shows the coefficient of correlation as 0.999, proving that the model reasonably reproduced the observed water chemistry.

Table 4 contains results from the mass balance. As can be seen, the amount of dissolved albite almost equals

that of gibbsite that precipitates, indicating an inverse process. However, the (slight) discrepancy between the Na^+ content generated by the model and the observed one (see also **Table 3**) suggests other sources of Na in solution, like cationic exchange process. In contrast to Na, predicted and observed concentration for both Ca and Mg match quite well.

Moreover, **Table 4** provides an estimate of the contribution of dissolved CO_2 to alkalinity ($\text{H}_2\text{CO}_3 \leftrightarrow \text{H}^+ + \text{HCO}_3^-$). The value so determined is 2.27 mmol/L (99.88 mg C/L as CO_2), a plausible range of CO_2 gas in the soil zone [20]. For the studied case, input CO_2 gas provides nearly 42% of the total alkalinity source, which demonstrates its important role in the mineralization of groundwater in the considered system.

Overall, the stated mass balance would mean that the down-gradient well chemistry at sampling location Pr15 equals the up-gradient spring water chemistry at location Pr1 plus phases dissolving, minus phases precipitating. However, precipitation is negligible, as is the case for gibbsite (see List 1). For instance, the total alkalinity concentration (405.46 mg C/L) given in **Table 3** for sample Pr15 should be equal to the up-gradient carbon concentration of sample Pr1 (=14.13 mg C/L), plus the carbon from calcite and dolomite dissolution [$3.21 \text{ mmole CO}_3^{2-} \times 60 \text{ g/mole} = 192.6 \text{ mg C/L}$] plus the carbon from dissolution of aqueous CO_2 [$2 \times 2.27 \text{ mmole CO}_2 \times 44 \text{ g/mole} = 199.76 \text{ mg C/L}$] = 406.49 mg C/L. The two values agree well, as can be inferred from results of the mass balances calculations shown on **Table 4**.

Table 3. Set of element concentrations essential for corroborating model results.

Elements	Input solution (Pr1)	Model output	Obs. composition (Pr15)
	mg/L (mmol/L)	mg/L (mmol/L)	mg/L (mmol/L)
Ca	1.92 (4.79E-02)	86.80 (2.16E+00)	88.24 (2.20E+00)
Mg	0.51 (2.10E-02)	13.57 (5.59E-01)	13.47 (5.54E-01)
Na	0.28 (1.22E-02)	6.41 (2.79E-01)	9.51 (4.14E-01)
C (as CO_2)	14.13 (3.21E-01)	405.46 (9.22E+00)	408 (9.28E+00)
Si (as SiO_2)	16.77 (2.79E-01)	64.80 (1.08E+00)	57.12 (9.51E-01)
Al	0.02 (7.41E-04)	0.0010 (3.74E-05)	0.0010 (3.71E-05)

Note: The ionic increase from sample Pr1 to sample Pr15 was modeled (column 2) as evolutionary change in the aquifer due to a greater magnitude of water-mineral-interaction along flow path; essentially carbonate and silicate minerals.

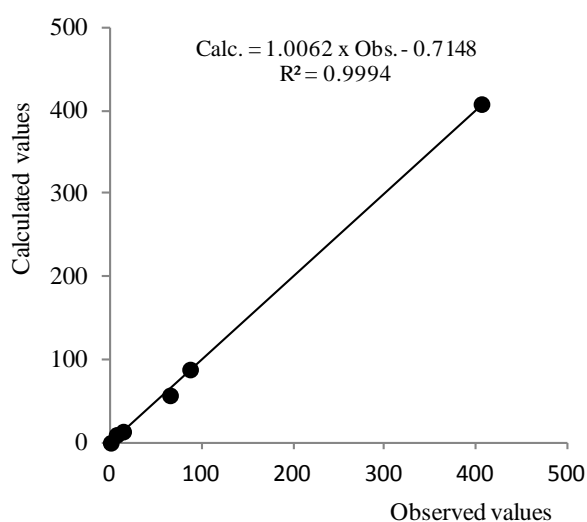


Figure 6. Correlation between the observed and modeled six elements' concentrations: Note: The fitted line is not statistically distinct from the line of one-to-one.

Table 4. Selected results from the mass balance calculations.

Selected data	Water sample		Mass transfer: Pr1 \Rightarrow Pr15
	Pr1	Pr15	
SI_{Albite}	-4.54	-1.86	$\Delta(SI) = 2.68$ (Albite dissolution = 2.667E-01 mmoles) $\Delta(\text{Na}^+)$: +9.23 mg/L (0.40 mmol/L)
SI_{Calcite}	-4.49	-0.53	$\Delta(SI) = 3.96$ (Calcite dissolution = 1.578E+00 mmoles) $\Delta(\text{Ca}^{2+})$: +86.32 mg/L (2.16 mmol/L)
SI_{Dolomite}	-9.28	-1.58	$\Delta(SI) = 7.70$ (Dolomite dissolution: 5.38 E-01 mmoles) $\Delta(\text{Mg}^{2+})$: +12.96 mg/L (0.53 mmol/L)
SI_{Gibbsite}	-1.11	-2.16	$\square \Delta(SI) = -1.05$ (Gibbsite precipitation: 2.67E-01 mmoles) $\Delta(\text{Al}^{3+})$: -0.019 mg/L (-0.0007 mmol/L)
SI_{CO_2}	-2.21	-1.04	$\Delta(SI) = 1.17$ ($\text{CO}_{2(\text{gas})}$ dissolution: 6.24E+00 mmoles)

$\Delta(\text{C/alkalinity as CO}_2)$: +393.87 mg C/L (+8.95 mmol C/L)

Balance calculation for total alkalinity

Change in alkalinity along flow path Pr1 \rightarrow Pr15: (HCO_3^-): +334.10 mg/L (+5.48 mmol/L)

CO_3^{2-} released from (Calcite + Dolomite) dissolution: 2.15 + 2*0.53 = 3.21 mmoles/L (192.60 mg/L)

$\Delta(\text{HCO}_3^-)$ from dissolution of $\text{CO}_2(\text{g})$ ($\text{H}_2\text{CO}_3 \rightleftharpoons \text{H}^+ + \text{HCO}_3^-$): 5.48 - 3.21 = 2.27 mmol/L (99.88 mg/L)

Alkalinity balance: 192.60 mg C as $\text{CO}_3^{2-}/\text{L}$ + (2*99.88 mg C as HCO_3^-/L) = **392.36 mg C/L (8.91 mmol C/L)**

Note: Changes in saturation state $\Delta(SI)$ indicate possible chemical reaction of the specific mineral phase in the aquifers. A positive value implies mineral dissolution and a negative value indicates mineral precipitation.

5. Conclusions

In terms of the interpretation of the major ion loading of groundwater in the DPA and the geochemical reactions paths modelling, the conclusions of this study are as follows:

1) Chemical data analysis through graphical plots and aqueous speciation calculations revealed that the predominant groundwater reactions were the carbon dioxide-driven processes of carbonate and silicate minerals weathering that produced the calcium-magnesium-bicarbonate and sodium-bicarbonate waters which showed near saturation with respect to the minerals calcite and dolomite and albite among others; and

2) The PHREEQC batch modelling, which simulated the observed flow path data, supported the hypotheses on the stages of hydrogeochemical evolution of groundwater.

Acknowledgements

The work benefitted significantly from discussions with Prof. Dr. F. Wisotzky of the RU Bochum (RFG), who we wish to thank.

References

[1] Garrels, R.M. and Mac Kenzie, F.T. (1967) Origin of the Chemical Compositions of Some Springs and Lakes. In:

- Gould, R.F., Ed., *Equilibrium Concepts in Natural Water Systems: Advances in Chemistry Series*, American Chemical Society, Washington DC, 222-242. <http://dx.doi.org/10.1021/ba-1967-0067.ch010>
- [2] Drever, J.I. (1988) *The Geochemistry of Natural Waters*. 2nd Edition, Prentice-Hall, Englewood Cliffs, 437 p.
- [3] Bricker, O.P., Godfrey, A. and Cleaves, E. (1968) Mineral-Water Interaction during the Chemical Weathering of Silicates. In: Baker, R.A., Ed., *Trace Inorganics in Water: Advances in Chemistry Series*, American Chemical Society, Washington DC, 128-142. <http://dx.doi.org/10.1021/ba-1968-0073.ch006>
- [4] Freeze, R.A. and Cherry, J.A. (1979) *Groundwater*. Prentice-Hall, Inc., Englewood Cliffs.
- [5] Polzer, W.L. and Hem, J.D. (1965) The Dissolution of Kaolinite. *Journal of Geophysical Research*, **70**, 6233-6240. <http://dx.doi.org/10.1029/JZ070i024p06233>
- [6] Hem, J. (1977) Surface Chemical Processes in Groundwater Systems. *Proceedings of the Second International Symposium on Water-Rock Interaction*, Strasbourg, 17-25 August 1977, IV 76-IV 85.
- [7] Tardy, Y. (1971) Characterization of the Principal Weathering Types by the Geochemistry of Waters from Some European and African Crystalline Massifs. *Chemical Geology*, **7**, 253-271. [http://dx.doi.org/10.1016/0009-2541\(71\)90011-8](http://dx.doi.org/10.1016/0009-2541(71)90011-8)
- [8] White, D.E., Hem, J.D. and Waring, G.A. (1963) Chemical Composition of Subsurface Waters. In: *Data of Geochemistry*, 6th Edition, US Geological Survey Professional Paper 440-F, 67 p.
- [9] Diop, S., Diome, F., Samb, M. and Sarr, R. (2014) Hydrogeochemical Relationships between Spring and Subsurface Waters in the Dindéfello Area of South Eastern Senegal. *Journal of Water Resource and Protection*, **6**.
- [10] Parkhurst, D.L. and Apello, C.A.J. (1999) User's Guide to PHREEQC (Version 2)—A Computer Program for Speciation, Batch Reaction, One Dimensional Transport and Inverse Geochemical Calculations. US Department of the Interior, USGS, Water Resource Investigations—Report No. 99-4259, Denver Colorado.
- [11] Le Page, A. (1986) The Main Geological Units of the Mauritanides Belt at the Senegal-Mauritanian Borders—Structural Changes in the Chain from Upper Precambrian to Devonian. Thèse de Doctorat d'Etat, Université Aix-Marseille, Marseille, 518 p.
- [12] Le Page, A. (1988) Rock Deformation Associated with the Displacement of Allochthonous Units in the Central Segment of the Caledono-Hercynian Mauritanides Belt (Islamic Republic of Mauritania and Eastern Senegal). *Journal of African Earth Sciences*, **7**, 265-283.
- [13] Lecorche, J.-P. and Sougy, J. (1978) The Mauritanides, West Africa, a Synthesis Assay. PIGC-UNESCO Project No. 27, Caledonide Orogen, Geological Survey of Canada, Ottawa.
- [14] Mischar, A. and Sougy, J. (1978) The Hercynian Orogen in the Northwestern Edge of Africa (Structures of the Primary Chains from Morocco to Senegal). *Proceedings of the Colloque Intern. CNRS No. 243, The Variscan Chain of Mid and Western Europe*, Rennes, 27 September-6 October 1978, 604-640.
- [15] Bassot, J.P. (1966) Geological Study of Eastern Senegal and Its Guinea-Malian Borders. *Mémoires du BRGM*, **40**, 322 p.
- [16] Villeneuve, M. (1984) Geological Study of the SW Border of the West African Craton—The Pan-African Suture and the Evolution of the Proterozoic—Paleozoic Sedimentary Basins on the NW Gondwana Margin. Thèse Doctorat d'Etat, Université d'Aix-Marseille III, Marseille, 552 p.
- [17] Villeneuve, M. (1989) The Geology of the Madina Kouta Basin (Guinea-Senegal) and Its Significance for the Geodynamic Evolution of the Western Part of the West African Craton during the Upper Proterozoic Period. *Precambrian Research*, **44**, 305-322. [http://dx.doi.org/10.1016/0301-9268\(89\)90050-8](http://dx.doi.org/10.1016/0301-9268(89)90050-8)
- [18] Delor, C., Couéffé, R., Goujou, J.-C., Diallo, D.P., Théveniaut, H., Fullgraf, T., Ndiaye, P.M., Dioh, E., Blein, O., Barry, T.M.M., Cocherie, A., Le Métour, J., Martelet, G., Sergeev, S. and Wemmer, K. (2010) Explanatory Notes to the 1/200,000 Geological Map of Senegal, Saraya-East Kédougou Sheet. Ministère des Mines, de l'Industrie, de l'Agro-Industrie et des PME, DMG, Dakar, 195 p.
- [19] Diop, S. (1998) Contribution to the Hydrogeology of the Fractured Aquifers Developed within the Crystalline Area of Eastern Senegal: Isotope-Hydrogeochemical Investigations and Water Balances in the Kédougou Area (Districts of Bandafassi, Salémata, Fongolimbi and Saraya). *Münster Forsch Geol Paläont*, **84**, 175-259.
- [20] Lee, R.W. (1985) Geochemistry of Groundwater in Cretaceous Sediments of the Southeastern Coastal Plain of Eastern Mississippi and Western Alabama. *Water Resources Research*, **21**, 1545-1556. <http://dx.doi.org/10.1029/WR021i010p01545>
- [21] Plummer, N., Busby, J.F., Lee, R.W. and Hanshaw, B.B. (1990) Geochemical Modeling of the Madison Aquifer in Parts of Montana, Wyoming and South Dakota. *Water Resources Research*, **26**, 1981-2014. <http://dx.doi.org/10.1029/WR026i009p01981>
- [22] Travi, Y., Gac, J.Y., Fontes, J.C. and Fritz, B. (1987) Reconnaissance Chimique et Isotopique des Eaux de Pluies au

Sénégal (A Survey of the Chemical and Isotopic Composition of Rainwater in Senegal). *Géodynamique*, **2**, 43-53.

- [23] Krauskopf, K.B. (1967) Introduction to Geochemistry. McGraw-Hill, Inc., New York, St Louis, San Francisco, Toronto, London and Sydney, 721 p.
- [24] Garrels, R.M. and Christ, C.L. (1965) Solutions, Minerals and Equilibria. W. H. Freeman, San Francisco, 450 p.

Appendix

In this appendix details are given of the model implementation and output result (List 1, below). More details on the computation procedure can be found in the tutorial [9].

The heading “Reading data base” (Bloc 1) defines the algorithms here used for simulating the reactions path. The heading “Reading input data for simulation 1” (Bloc 2) introduces the essential data supplied to the model, namely: the initial solution (SOLUTION 1), representing hereinafter water sample Pr1 and the set of phases (“EQUILIBRIUM PHASES 1”) that are supposed to react during the batch reaction to turn the initial solution to a mineral saturation state matching that of water sample Pr15 (final solution). Thus, the keyword “SOLUTION 1” defines the composition of sample Pr1 and “EQUILIBRIUM PHASES 1” is the keyword that declares the list of phases used in the model and their respective SI. These so-called “target SIs values” were anticipated from a PHREEQC speciation of water sample Pr15. They are entered in the model to thermodynamically constraints the system. So conceptually, we consider the chemical balance that would result if water sample Pr1 were placed in a beaker which is regulated at 20°C and allowed to react with the specified minerals and gas phases until the saturation limits are attained.

“Beginning of initial solution calculations” (Bloc 3) specifies the conversion of the input concentration data for Pr1 into molality (subheading “solution composition”). Subheading “Description of solution” introduces some basic properties calculated by the model. Subheading “Distribution of species” lists the different elements (master species) and amount of corresponding aqueous species in the solution. Subheading “Saturation indices” lists the SI calculations for all minerals that are appropriate for the aqueous solution and their respective formula.

The heading “Beginning of the batch reaction” (Bloc 4) defines the beginning of the batch reaction calculations for the simulation. When the simulation begins the initial solution and pure phases are put together and allowed to react until the saturation limits utilized to thermodynamically constraint the system (stated target SI values) are attained. The proportion of reactant is one mole for each mineral phase.

After the calculations are completed, the numbers of moles consumed for the reactions (mass transfers) are presented under subheading “Phase assemblage” (see Bloc 4.1; whereby positive delta value indicates precipitation and negative delta value dissolution). The resulting water chemistry (output or final solution) is then computed the (see subheading “Solution composition”; Bloc 4.2). Next, PRHEEQC calculates the resultant aqueous speciation (see subheading “Distribution of species”, Bloc 4.4) and then provides SIs for possible and impossible sources or sinks of solutes (see Subheading “Saturation indices”, Bloc 4.5).

List 1: Output data file for the modeled flow path

```
Input file: phreeqc.tmp
Output file: C:\Programme\Phreeqc\senegall.out
Database file: C:\Programme\Phreeqc\Phreeqc.dat
```

```
-----
Reading data base.          (BLOC 1)
-----
```

```
SOLUTION_MASTER_SPECIES
  SOLUTION_SPECIES
  PHASES
  EXCHANGE_MASTER_SPECIES
  EXCHANGE_SPECIES
  SURFACE_MASTER_SPECIES
  SURFACE_SPECIES
  RATES
  END
```

```
-----
Reading input data for simulation 1.  (BLOC 2)
```

 TITLE Analyse Senegal Pr. 1 (BLOC 2.1)

SOLUTION 1

units mg/l

pH 5.89

pe 4.0

density 1.000

temp 20.0 # estimated

Ca²⁺ 1.92

Mg²⁺ 0.51

Na⁺ 0.28

K⁺ 0.43

Fe²⁺ 0.001

Mn²⁺ 0.001

Sr²⁺ 0.001

Cl⁻ 0.98

C 14.13 as CO₂ # from ionic balance

S⁶⁺ 1.27

N⁵⁺ 1.43 as NO₃⁻

Si⁴⁺ 16.77 as SiO₂

Al³⁺ 0.02

B³⁺ 0.22

EQUILIBRIUM_PHASES 1 (BLOC 2.2)

Calcite -0.53

Dolomite -1.58

Albite -1.86

Al(OH)₃(a) -2.16

CO₂(g) -1.04

END

 TITLE Analyse Senegal Diop Pr. 1

 Beginning of initial solution calculations. (BLOC 3)

Initial solution 1.

-----Solution composition----- (BLOC 3.1)-----

Elements	Molality	Moles
Al ³⁺	7.413e-07	7.413e-07
B ³⁺	2.035e-05	2.035e-05
C ⁴⁺	3.211e-04	3.211e-04
Ca ²⁺	4.791e-05	4.791e-05
Cl ⁻	2.764e-05	2.764e-05
Fe ³⁺	1.791e-08	1.791e-08
K ⁺	1.100e-05	1.100e-05
Mg ²⁺	2.098e-05	2.098e-05
Mn ²⁺	1.820e-08	1.820e-08

N ⁵⁺	2.306e-05	2.306e-05
Na ⁺	1.218e-05	1.218e-05
S ⁶⁺	1.322e-05	1.322e-05
Si ⁴⁺	2.791e-04	2.791e-04
Sr ²⁺	1.141e-08	1.141e-08

-----Description of solution----- (BLOC 3.2)-----

pH = 5.890
 pe = 4.000
 Activity of water = 1.000
 Ionic strength = 2.415e-04
 Mass of water (kg) = 1.000e+00
 Total alkalinity (eq/kg) = 7.951e-05
 Total CO2 (mol/kg) = 3.211e-04
 Temperature (deg C) = 20.000
 Electrical balance (eq) = 6.611e-06
 Percent error, 100*(Cat-|An|)/(Cat+|An|) = 2.07
 Iterations = 10
 Total H = 1.110137e+02
 Total O = 5.550824e+01

-----Distribution of species----- (BLOC 3.3)-----

Species	Molality	Log Activity	Log Molality	Log Activity	Gamma
H ⁺	1.311e-06	1.288e-06	-5.882	-5.890	-0.008
OH ⁻	5.364e-09	5.270e-09	-8.270	-8.278	-0.008
H ₂ O	5.551e+01	1.000e+00	1.744	-0.000	0.000
Al	7.413e-07				
Al(OH) ₂ ⁺	4.905e-07	4.819e-07	-6.309	-6.317	-0.008
AlOH ²⁺	1.333e-07	1.242e-07	-6.875	-6.906	-0.031
Al(OH) ₄ ⁻	5.279e-08	5.186e-08	-7.277	-7.285	-0.008
Al(OH) ₃	3.767e-08	3.767e-08	-7.424	-7.424	0.000
Al ⁺³	2.614e-08	2.238e-08	-7.583	-7.650	-0.068
AlSO ₄ ⁺	8.210e-10	8.066e-10	-9.086	-9.093	-0.008
Al(SO ₄) ₂ ⁻	3.087e-13	3.033e-13	-12.510	-12.518	-0.008
AlHSO ₄ ²⁺	9.493e-17	8.844e-17	-16.023	-16.053	-0.031
B	2.035e-05				
H ₃ BO ₃	2.034e-05	2.035e-05	-4.692	-4.692	0.000
H ₂ BO ₃ ⁻	8.430e-09	8.282e-09	-8.074	-8.082	-0.008
C(-4)	0.000e+00				
CH ₄	0.000e+00	0.000e+00	-57.660	-57.660	0.000
C(4)	3.211e-04				
CO ₂	2.417e-04	2.417e-04	-3.617	-3.617	0.000
HCO ₃ ⁻	7.927e-05	7.789e-05	-4.101	-4.109	-0.008
CaHCO ₃ ⁺	4.136e-08	4.064e-08	-7.383	-7.391	-0.008
MgHCO ₃ ⁺	1.773e-08	1.742e-08	-7.751	-7.759	-0.008
CO ₃ ²⁻	2.732e-09	2.546e-09	-8.564	-8.594	-0.031
NaHCO ₃	5.241e-10	5.241e-10	-9.281	-9.281	0.000
CaCO ₃	1.738e-10	1.738e-10	-9.760	-9.760	0.000
FeHCO ₃ ⁺	1.310e-10	1.287e-10	-9.883	-9.890	-0.008
MnHCO ₃ ⁺	1.189e-10	1.168e-10	-9.925	-9.933	-0.008
MgCO ₃	4.386e-11	4.386e-11	-10.358	-10.358	0.000

SrHCO ₃ ⁺	1.084e-11	1.065e-11	-10.965	-10.973	-0.008
MnCO ₃	3.402e-12	3.403e-12	-11.468	-11.468	0.000
FeCO ₃	1.009e-12	1.010e-12	-11.996	-11.996	0.000
NaCO ₃ ⁻	4.468e-13	4.390e-13	-12.350	-12.358	-0.008
SrCO ₃	1.487e-14	1.487e-14	-13.828	-13.828	0.000
Ca	4.791e-05				
Ca ²⁺	4.776e-05	4.451e-05	-4.321	-4.352	-0.031
CaSO ₄	1.031e-07	1.031e-07	-6.987	-6.987	0.000
CaHCO ₃ ⁺	4.136e-08	4.064e-08	-7.383	-7.391	-0.008
CaCO ₃	1.738e-10	1.738e-10	-9.760	-9.760	0.000
CaOH ⁺	5.837e-12	5.734e-12	-11.234	-11.242	-0.008
CaHSO ₄ ⁺	7.465e-13	7.334e-13	-12.127	-12.135	-0.008
Cl	2.764e-05				
Cl ⁻	2.764e-05	2.716e-05	-4.558	-4.566	-0.008
MnCl ⁺	1.894e-12	1.861e-12	-11.723	-11.730	-0.008
FeCl ⁺	6.306e-13	6.196e-13	-12.200	-12.208	-0.008
MnCl ₂	2.206e-17	2.206e-17	-16.656	-16.656	0.000
FeCl ²⁺	8.950e-21	8.338e-21	-20.048	-20.079	-0.031
MnCl ₃ ⁻	1.680e-22	1.650e-22	-21.775	-21.782	-0.008
FeCl ₂ ⁺	1.210e-24	1.188e-24	-23.917	-23.925	-0.008
FeCl ₃	3.227e-30	3.227e-30	-29.491	-29.491	0.000
Fe (2)	1.790e-08				
Fe ²⁺	1.773e-08	1.653e-08	-7.751	-7.782	-0.030
FeHCO ₃ ⁺	1.310e-10	1.287e-10	-9.883	-9.890	-0.008
FeSO ₄	3.260e-11	3.261e-11	-10.487	-10.487	0.000
FeOH ⁺	2.824e-12	2.774e-12	-11.549	-11.557	-0.008
FeCO ₃	1.009e-12	1.010e-12	-11.996	-11.996	0.000
FeCl ⁺	6.306e-13	6.196e-13	-12.200	-12.208	-0.008
FeHSO ₄ ⁺	2.772e-16	2.723e-16	-15.557	-15.565	-0.008
Fe (3)	1.038e-11				
Fe(OH) ₂ ⁺	9.574e-12	9.406e-12	-11.019	-11.027	-0.008
Fe(OH) ₃	7.535e-13	7.536e-13	-12.123	-12.123	0.000
FeOH ²⁺	4.764e-14	4.438e-14	-13.322	-13.353	-0.031
Fe(OH) ₄ ⁻	4.426e-16	4.349e-16	-15.354	-15.362	-0.008
Fe ³⁺	1.396e-17	1.194e-17	-16.855	-16.923	-0.068
FeSO ₄ ⁺	1.450e-18	1.425e-18	-17.839	-17.846	-0.008
FeCl ²⁺	8.950e-21	8.338e-21	-20.048	-20.079	-0.031
Fe(SO ₄) ₂ ⁻	3.787e-22	3.721e-22	-21.422	-21.429	-0.008
FeHSO ₄ ²⁺	5.307e-24	4.944e-24	-23.275	-23.306	-0.031
FeCl ₂ ⁺	1.210e-24	1.188e-24	-23.917	-23.925	-0.008
Fe ₂ (OH) ₂ ⁴⁺	8.683e-26	6.540e-26	-25.061	-25.184	-0.123
FeCl ₃	3.227e-30	3.227e-30	-29.491	-29.491	0.000
Fe ₃ (OH) ₄ ⁵⁺	3.199e-34	2.055e-34	-33.495	-33.687	-0.192
H(0)	2.378e-23				
H ₂	1.189e-23	1.189e-23	-22.925	-22.925	0.000
K	1.100e-05				
K ⁺	1.100e-05	1.080e-05	-4.959	-4.966	-0.008
KSO ₄ ⁻	8.608e-10	8.457e-10	-9.065	-9.073	-0.008
KOH	2.907e-14	2.908e-14	-13.536	-13.536	0.000
Mg	2.098e-05				
Mg ²⁺	2.091e-05	1.949e-05	-4.680	-4.710	-0.030
MgSO ₄	4.880e-08	4.881e-08	-7.312	-7.312	0.000
MgHCO ₃ ⁺	1.773e-08	1.742e-08	-7.751	-7.759	-0.008

MgCO ₃	4.386e-11	4.386e-11	-10.358	-10.358	0.000
MgOH ⁺	3.533e-11	3.471e-11	-10.452	-10.460	-0.008
Mn(2)	1.820e-08				
Mn ²⁺	1.805e-08	1.682e-08	-7.744	-7.774	-0.030
MnHCO ₃ ⁺	1.189e-10	1.168e-10	-9.925	-9.933	-0.008
MnSO ₄	3.305e-11	3.306e-11	-10.481	-10.481	0.000
MnCO ₃	3.402e-12	3.403e-12	-11.468	-11.468	0.000
MnCl ⁺	1.894e-12	1.861e-12	-11.723	-11.730	-0.008
MnOH ⁺	2.257e-13	2.218e-13	-12.646	-12.654	-0.008
Mn(NO ₃) ₂	3.477e-17	3.477e-17	-16.459	-16.459	0.000
MnCl ₂	2.206e-17	2.206e-17	-16.656	-16.656	0.000
MnCl ₃ ⁻	1.680e-22	1.650e-22	-21.775	-21.782	-0.008
Mn(3)	2.901e-30				
Mn ³⁺	2.901e-30	2.474e-30	-29.537	-29.607	-0.069
N(5)	2.306e-05				
NO ₃ ⁻	2.306e-05	2.266e-05	-4.637	-4.645	-0.008
Mn(NO ₃) ₂	3.477e-17	3.477e-17	-16.459	-16.459	0.000
Na	1.218e-05				
Na ⁺	1.218e-05	1.197e-05	-4.914	-4.922	-0.008
NaSO ₄ ⁻	7.196e-10	7.070e-10	-9.143	-9.151	-0.008
NaHCO ₃	5.241e-10	5.241e-10	-9.281	-9.281	0.000
NaCO ₃ ⁻	4.468e-13	4.390e-13	-12.350	-12.358	-0.008
NaOH	6.136e-14	6.136e-14	-13.212	-13.212	0.000
O(0)	0.000e+00				
O ₂	0.000e+00	0.000e+00	-48.205	-48.205	0.000
S(6)	1.322e-05				
SO ₄ ²⁻	1.307e-05	1.218e-05	-4.884	-4.915	-0.031
CaSO ₄	1.031e-07	1.031e-07	-6.987	-6.987	0.000
MgSO ₄	4.880e-08	4.881e-08	-7.312	-7.312	0.000
HSO ₄ ⁻	1.395e-09	1.370e-09	-8.855	-8.863	-0.008
KSO ₄ ⁻	8.608e-10	8.457e-10	-9.065	-9.073	-0.008
AlSO ₄ ⁺	8.210e-10	8.066e-10	-9.086	-9.093	-0.008
NaSO ₄ ⁻	7.196e-10	7.070e-10	-9.143	-9.151	-0.008
MnSO ₄	3.305e-11	3.306e-11	-10.481	-10.481	0.000
FeSO ₄	3.260e-11	3.261e-11	-10.487	-10.487	0.000
SrSO ₄	2.371e-11	2.371e-11	-10.625	-10.625	0.000
CaHSO ₄ ⁺	7.465e-13	7.334e-13	-12.127	-12.135	-0.008
Al(SO ₄) ₂ ⁻	3.087e-13	3.033e-13	-12.510	-12.518	-0.008
FeHSO ₄ ⁺	2.772e-16	2.723e-16	-15.557	-15.565	-0.008
AlHSO ₄ ²⁺	9.493e-17	8.844e-17	-16.023	-16.053	-0.031
FeSO ₄ ⁺	1.450e-18	1.425e-18	-17.839	-17.846	-0.008
Fe(SO ₄) ₂ ⁻	3.787e-22	3.721e-22	-21.422	-21.429	-0.008
FeHSO ₄ ²⁺	5.307e-24	4.944e-24	-23.275	-23.306	-0.031
Si	2.791e-04				
H ₄ SiO ₄	2.791e-04	2.791e-04	-3.554	-3.554	0.000
H ₃ SiO ₄ ⁻	2.717e-08	2.669e-08	-7.566	-7.574	-0.008
H ₂ SiO ₄ ²⁻	1.082e-15	1.008e-15	-14.966	-14.997	-0.031
Sr	1.141e-08				
Sr ²⁺	1.138e-08	1.061e-08	-7.944	-7.974	-0.031
SrSO ₄	2.371e-11	2.371e-11	-10.625	-10.625	0.000
SrHCO ₃ ⁺	1.084e-11	1.065e-11	-10.965	-10.973	-0.008
SrCO ₃	1.487e-14	1.487e-14	-13.828	-13.828	0.000
SrOH ⁺	4.297e-16	4.222e-16	-15.367	-15.374	-0.008

-----Saturation indices----- **BLOC 3.4**-----

Phase	SI	log IAP	log KT	
Al(OH) ₃ (a)	-1.11	10.02	11.13	Al(OH) ₃
Albite	-4.54	-22.87	-18.33	NaAlSi ₃ O ₈
Alunite	-1.63	-2.41	-0.77	KAl ₃ (SO ₄) ₂ (OH) ₆
Anhydrite	-4.92	-9.27	-4.34	CaSO ₄
Anorthite	-6.17	-26.03	-19.86	CaAl ₂ Si ₂ O ₈
Aragonite	-4.64	-12.95	-8.31	CaCO ₃
Ca-Montmorillonite	3.24	-42.52	-45.76	Ca _{0.165} Al _{2.33} Si _{3.67} O ₁₀ (OH) ₂
Calcite	-4.49	-12.95	-8.45	CaCO ₃
Celestite	-6.27	-12.89	-6.62	SrSO ₄
CH ₄ (g)	-54.86	-57.66	-2.80	CH ₄
Chalcedony	0.06	-3.55	-3.61	SiO ₂
Chlorite(14A)	-25.55	44.73	70.27	Mg ₅ Al ₂ Si ₃ O ₁₀ (OH) ₈
Chrysotile	-18.73	14.10	32.83	Mg ₃ Si ₂ O ₅ (OH) ₄
CO ₂ (g)	-2.21	-3.62	-1.41	CO ₂
Dolomite	-9.28	-26.25	-16.97	CaMg(CO ₃) ₂
Fe(OH) ₃ (a)	-4.14	0.75	4.89	Fe(OH) ₃
Gibbsite	1.62	10.02	8.40	Al(OH) ₃
Goethite	1.57	0.75	-0.82	FeOOH
Gypsum	-4.68	-9.27	-4.58	CaSO ₄ ·2H ₂ O
H ₂ (g)	-19.73	24.10	43.83	H ₂
H ₂ O(g)	-1.64	-0.00	1.64	H ₂ O
Halite	-11.06	-9.49	1.57	NaCl
Hausmannite	-30.49	31.80	62.29	Mn ₃ O ₄
Hematite	5.12	1.49	-3.62	Fe ₂ O ₃
Illite	0.53	-40.42	-40.95	K _{0.6} Mg _{0.25} Al _{2.3} Si _{3.5} O ₁₀ (OH) ₂
Jarosite-K	-21.41	-30.22	-8.82	KFe ₃ (SO ₄) ₂ (OH) ₆
K-feldspar	-1.96	-22.91	-20.96	KAlSi ₃ O ₈
K-mica	6.87	20.32	13.45	KAl ₃ Si ₃ O ₁₀ (OH) ₂
Kaolinite	5.05	12.93	7.88	Al ₂ Si ₂ O ₅ (OH) ₄
Manganite	-11.44	13.90	25.34	MnOOH
Melanterite	-10.42	-12.70	-2.27	FeSO ₄ ·7H ₂ O
O ₂ (g)	-45.35	-48.21	-2.85	O ₂
Pyrochroite	-11.19	4.01	15.20	Mn(OH) ₂
Pyrolusite	-18.41	23.79	42.19	MnO ₂ ·H ₂ O
Quartz	0.48	-3.55	-4.04	SiO ₂
Rhodochrosite	-5.26	-16.37	-11.11	MnCO ₃
Sepiolite	-12.42	3.48	15.89	Mg ₂ Si ₃ O _{7.5} OH·3H ₂ O
Sepiolite(d)	-15.18	3.48	18.66	Mg ₂ Si ₃ O _{7.5} OH·3H ₂ O
Siderite	-5.52	-16.38	-10.86	FeCO ₃
SiO ₂ (a)	-0.80	-3.55	-2.75	SiO ₂
Strontianite	-7.30	-16.57	-9.27	SrCO ₃
Talc	-14.99	6.99	21.98	Mg ₃ Si ₄ O ₁₀ (OH) ₂

Beginning of batch-reaction calculations.**(BLOC 4)**

Reaction step 1.

Using solution 1.

Using pure phase assemblage 1.

-----Phase assemblage----- (BLOC4.1)---

Phase	SI	log IAP	log KT	Moles in assemblage		
				Initial	Final	Delta
Al(OH) ₃ (a)	-2.16	8.97	11.13	1.000e+01	1.000e+01	2.674e-04
Albite	-1.86	-20.19	-18.33	1.000e+01	1.000e+01	-2.667e-04
Calcite	-0.53	-8.98	-8.45	1.000e+01	9.998e+00	-1.578e-03
CO ₂ (g)	-1.04	-2.45	-1.41	1.000e+01	9.994e+00	-6.240e-03
Dolomite	-1.58	-18.55	-16.97	1.000e+01	9.999e+00	-5.376e-04

-----Solution composition----- (BLOC4.2) --

Elements	Output(Moles)	Pr 15(Moles)
Al ³⁺	3.739e-08	3.708e-08
B ³⁺	2.035e-05	9.256e-08
C ⁴⁺	9.215e-03	9.276e-03
Ca ²⁺	2.164e-03	2.203e-03
Cl ⁻	2.765e-05	9.314e-05
Fe ²⁺	1.791e-08	1.792e-08
K ⁺	1.100e-05	2.303e-05
Mg ²⁺	5.586e-04	5.544e-04
Mn ²⁺	1.820e-08	1.821e-08
N ⁵⁺	2.306e-05	1.055e-04
Na ⁺	2.789e-04	4.139e-04
S ³⁺ (6)	1.322e-05	3.281e-05
Si ⁴⁺	1.079e-03	9.512e-04
Sr ²⁺	1.141e-08	2.741e-06

-----Description of solution----- (BLOC4.3) -----

pH = 6.532 Charge balance
 pe = 13.188 Adjusted to redox equilibrium
 Activity of water = 1.000
 Ionic strength = 8.219e-03
 Mass of water (kg) = 9.999e-01
 Total alkalinity (eq/kg) = 5.651e-03
 Total CO₂ (mol/kg) = 9.215e-03
 Temperature (deg C) = 20.000
 Electrical balance (eq) = 6.611e-06
 Percent error (Cat-|An|)/(Cat+|An|) = 0.06
 Iterations = 19
 Total H = 1.110129e+02
 Total O = 5.553001e+01

-----Distribution of species----- (BLOC4.4) -----

Species	Molality	Log	Log	Log	Gamma
		Activity	Molality	Activity	
H ⁺	3.193e-07	2.938e-07	-6.496	-6.532	-0.036
OH ⁻	2.542e-08	2.310e-08	-7.595	-7.636	-0.041
H ₂ O	5.551e+01	9.998e-01	1.744	-0.000	0.000

Al	3.739e-08				
Al(OH) ₄ ⁻	2.233e-08	2.033e-08	-7.651	-7.692	-0.041
Al(OH) ₂ ⁺	1.080e-08	9.833e-09	-7.967	-8.007	-0.041
Al(OH) ₃	3.363e-09	3.370e-09	-8.473	-8.472	0.001
Al(OH) ⁺²	8.412e-10	5.780e-10	-9.075	-9.238	-0.163
Al ⁺³	5.024e-11	2.376e-11	-10.299	-10.624	-0.325
AlSO ₄ ⁺	5.689e-13	5.179e-13	-12.245	-12.286	-0.041
Al(SO ₄) ₂ ⁻	1.294e-16	1.178e-16	-15.888	-15.929	-0.041
Al(HSO ₄) ₂ ²⁺	1.885e-20	1.295e-20	-19.725	-19.888	-0.163
B	2.035e-05				
H ₃ BO ₃	2.031e-05	2.035e-05	-4.692	-4.691	0.001
H ₂ BO ₃ ⁻	3.990e-08	3.633e-08	-7.399	-7.440	-0.041
C(-4)	0.000e+00				
CH ₄	0.000e+00	0.000e+00	-135.128	-135.127	0.001
C ⁴⁺ (4)	9.215e-03				
HCO ₃ ⁻	5.528e-03	5.048e-03	-2.257	-2.297	-0.039
CO ₂	3.567e-03	3.574e-03	-2.448	-2.447	0.001
Ca(HCO ₃) ⁺	9.305e-05	8.497e-05	-4.031	-4.071	-0.039
Mg(HCO ₃) ⁺	2.373e-05	2.161e-05	-4.625	-4.665	-0.041
CaCO ₃	1.591e-06	1.594e-06	-5.798	-5.798	0.001
CO ₃ ²⁻	1.041e-06	7.235e-07	-5.983	-6.141	-0.158
NaHCO ₃	7.182e-07	7.19e-07	-6.144	-6.143	0.001
MgCO ₃	2.381e-07	2.385e-07	-6.623	-6.622	0.001
MnHCO ₃ ⁺	4.536e-09	4.129e-09	-8.343	-8.384	-0.041
NaCO ₃ ⁻	2.903e-09	2.643e-09	-8.537	-8.578	-0.041
SrHCO ₃ ⁺	5.387e-10	4.919e-10	-9.269	-9.308	-0.039
MnCO ₃	5.265e-10	5.275e-10	-9.279	-9.278	0.001
SrCO ₃	3.007e-12	3.012e-12	-11.522	-11.521	0.001
FeHCO ₃ ⁺	4.060e-16	3.696e-16	-15.391	-15.432	-0.041
FeCO ₃	1.269e-17	1.271e-17	-16.897	-16.896	0.001
Ca	2.164e-03				
Ca ²⁺	2.067e-03	1.436e-03	-2.685	-2.843	-0.158
CaHCO ₃ ⁺	9.305e-05	8.497e-05	-4.031	-4.071	-0.039
CaSO ₄	2.009e-06	2.012e-06	-5.697	-5.696	0.001
CaCO ₃	1.591e-06	1.594e-06	-5.798	-5.798	0.001
CaOH ⁺	8.909e-10	8.111e-10	-9.050	-9.091	-0.041
CaHSO ₄ ⁺	3.585e-12	3.264e-12	-11.445	-11.486	-0.041
Cl	2.765e-05				
Cl ⁻	2.765e-05	2.513e-05	-4.558	-4.600	-0.041
MnCl ⁺	1.032e-12	9.399e-13	-11.986	-12.027	-0.041
MnCl ₂	1.029e-17	1.031e-17	-16.987	-16.987	0.001
FeCl ⁺²	7.667e-19	5.268e-19	-18.115	-18.278	-0.163
FeCl ⁺	2.791e-20	2.541e-20	-19.554	-19.595	-0.041
MnCl ₃ ⁻	7.841e-23	7.139e-23	-22.106	-22.146	-0.041
FeCl ₂ ⁺	7.633e-23	6.949e-23	-22.117	-22.158	-0.041
FeCl ₃	1.743e-28	1.747e-28	-27.759	-27.758	0.001
Fe(2)	1.468e-15				
Fe ²⁺	1.047e-15	7.323e-16	-14.980	-15.135	-0.155
FeHCO ₃ ⁺	4.060e-16	3.696e-16	-15.391	-15.432	-0.041
FeCO ₃	1.269e-17	1.271e-17	-16.897	-16.896	0.001
FeSO ₄	8.721e-19	8.737e-19	-18.059	-18.059	0.001
FeOH ⁺	5.919e-19	5.389e-19	-18.228	-18.269	-0.041
FeCl ⁺	2.791e-20	2.541e-20	-19.554	-19.595	-0.041

FeHSO ₄ ⁺	1.828e-24	1.664e-24	-23.738	-23.779	-0.041
Fe(HS) ₂	0.000e+00	0.000e+00	-276.226	-276.225	0.001
Fe(HS) ₃ ⁻	0.000e+00	0.000e+00	-409.167	-409.208	-0.041
Fe(3)	1.791e-08				
Fe(OH) ₂ ⁺	1.355e-08	1.234e-08	-7.868	-7.909	-0.041
Fe(OH) ₃	4.325e-09	4.333e-09	-8.364	-8.363	0.001
Fe(OH) ₂ ²⁺	1.933e-11	1.328e-11	-10.714	-10.877	-0.163
Fe(OH) ₄ ⁻	1.204e-11	1.096e-11	-10.919	-10.960	-0.041
Fe ³⁺	1.724e-15	8.154e-16	-14.763	-15.089	-0.325
FeSO ₄ ⁺	6.461e-17	5.883e-17	-16.190	-16.230	-0.041
FeCl ²⁺	7.667e-19	5.268e-19	-18.115	-18.278	-0.163
Fe ₂ (OH) ₂ ⁴⁺	2.627e-20	5.857e-21	-19.581	-20.232	-0.652
Fe(SO ₄) ₂ ⁻	1.020e-20	9.290e-21	-19.991	-20.032	-0.041
FeCl ²⁺	7.633e-23	6.949e-23	-22.117	-22.158	-0.041
FeHSO ₄ ²⁺	6.775e-23	4.655e-23	-22.169	-22.332	-0.163
Fe ₃ (OH) ₄ ⁵⁺	2.519e-25	2.414e-26	-24.599	-25.617	-1.018
FeCl ₃	1.743e-28	1.747e-28	-27.759	-27.758	0.001
H(0)	0.000e+00				
H ₂	0.000e+00	0.000e+00	-42.585	-42.584	0.001
K	1.100e-05				
K ⁺	1.100e-05	9.999e-06	-4.959	-5.000	-0.041
KSO ₄ ⁻	5.200e-10	4.734e-10	-9.284	-9.325	-0.041
KOH	1.177e-13	1.180e-13	-12.929	-12.928	0.001
Mg	5.586e-04				
Mg ²⁺	5.341e-04	3.731e-04	-3.272	-3.428	-0.156
MgHCO ₃ ⁺	2.373e-05	2.161e-05	-4.625	-4.665	-0.041
MgSO ₄	5.639e-07	5.650e-07	-6.249	-6.248	0.001
MgCO ₃	2.381e-07	2.385e-07	-6.623	-6.622	0.001
MgOH ⁺	3.199e-09	2.912e-09	-8.495	-8.536	-0.041
Mn(2)	1.820e-08				
Mn ²⁺	1.313e-08	9.179e-09	-7.882	-8.037	-0.155
MnHCO ₃ ⁺	4.536e-09	4.129e-09	-8.343	-8.384	-0.041
MnCO ₃	5.265e-10	5.275e-10	-9.279	-9.278	0.001
MnSO ₄	1.089e-11	1.091e-11	-10.963	-10.962	0.001
MnCl ⁺	1.032e-12	9.399e-13	-11.986	-12.027	-0.041
MnOH ⁺	5.826e-13	5.304e-13	-12.235	-12.275	-0.041
Mn(NO ₃) ₂	1.616e-17	1.620e-17	-16.791	-16.791	0.001
MnCl ₂	1.029e-17	1.031e-17	-16.987	-16.987	0.001
MnCl ₃ ⁻	7.841e-23	7.139e-23	-22.106	-22.146	-0.041
Mn(3)	4.838e-21				
Mn ³⁺	4.838e-21	2.080e-21	-20.315	-20.682	-0.367
N(0)	4.616e-09				
N ₂	2.308e-09	2.312e-09	-8.637	-8.636	0.001
N(3)	1.098e-15				
NO ₂ ⁻	1.098e-15	9.970e-16	-14.959	-15.001	-0.042
N(5)	2.306e-05				
NO ₃ ⁻	2.306e-05	2.093e-05	-4.637	-4.679	-0.042
Mn(NO ₃) ₂	1.616e-17	1.620e-17	-16.791	-16.791	0.001
Na	2.789e-04				
Na ⁺	2.782e-04	2.535e-04	-3.556	-3.596	-0.040
NaHCO ₃	7.182e-07	7.196e-07	-6.144	-6.143	0.001
NaSO ₄ ⁻	9.949e-09	9.059e-09	-8.002	-8.043	-0.041
NaCO ₃ ⁻	2.903e-09	2.643e-09	-8.537	-8.578	-0.041

NaOH	5.688e-12	5.699e-12	-11.245	-11.244	0.001
O(0)	2.591e-09				
O ₂	1.296e-09	1.298e-09	-8.888	-8.887	0.001
S(-2)	0.000e+00				
H ₂ S	0.000e+00	0.000e+00	-134.543	-134.542	0.001
HS ⁻	0.000e+00	0.000e+00	-134.978	-135.020	-0.041
S ²⁻	0.000e+00	0.000e+00	-141.398	-141.557	-0.159
Fe(HS) ₂	0.000e+00	0.000e+00	-276.226	-276.225	0.001
Fe(HS) ₃ ⁻	0.000e+00	0.000e+00	-409.167	-409.208	-0.041
S(6)	1.322e-05				
SO ₄ ²⁻	1.064e-05	7.363e-06	-4.973	-5.133	-0.160
CaSO ₄	2.009e-06	2.012e-06	-5.697	-5.696	0.001
MgSO ₄	5.639e-07	5.650e-07	-6.249	-6.248	0.001
NaSO ₄ ⁻	9.949e-09	9.059e-09	-8.002	-8.043	-0.041
KSO ₄ ⁻	5.200e-10	4.734e-10	-9.284	-9.325	-0.041
HSO ₄ ⁻	2.076e-10	1.890e-10	-9.683	-9.723	-0.041
MnSO ₄	1.089e-11	1.091e-11	-10.963	-10.962	0.001
SrSO ₄	1.020e-11	1.022e-11	-10.991	-10.990	0.001
CaHSO ₄ ⁺	3.585e-12	3.264e-12	-11.445	-11.486	-0.041
AlSO ₄ ⁺	5.689e-13	5.179e-13	-12.245	-12.286	-0.041
Al(SO ₄) ²⁻	1.294e-16	1.178e-16	-15.888	-15.929	-0.041
FeSO ₄ ⁺	6.461e-17	5.883e-17	-16.190	-16.230	-0.041
FeSO ₄	8.721e-19	8.737e-19	-18.059	-18.059	0.001
AlHSO ₄ ⁺²	1.885e-20	1.295e-20	-19.725	-19.888	-0.163
Fe(SO ₄) ²⁻	1.020e-20	9.290e-21	-19.991	-20.032	-0.041
FeHSO ₄ ⁺²	6.775e-23	4.655e-23	-22.169	-22.332	-0.163
FeHSO ₄ ⁺	1.828e-24	1.664e-24	-23.738	-23.779	-0.041
Si	1.079e-03				
H ₄ SiO ₄	1.079e-03	1.081e-03	-2.967	-2.966	0.001
H ₃ SiO ₄ ⁻	4.978e-07	4.532e-07	-6.303	-6.344	-0.041
H ₂ SiO ₄ ²⁻	1.092e-13	7.502e-14	-12.962	-13.125	-0.163
Sr	1.141e-08				
Sr ²⁺	1.086e-08	7.560e-09	-7.964	-8.121	-0.157
SrHCO ₃ ⁺	5.387e-10	4.919e-10	-9.269	-9.308	-0.039
SrSO ₄	1.020e-11	1.022e-11	-10.991	-10.990	0.001
SrCO ₃	3.007e-12	3.012e-12	-11.522	-11.521	0.001
SrOH ⁺	1.446e-15	1.319e-15	-14.840	-14.880	-0.040

-----Saturation indices----- (BLOC4.5) -----

Phase	SI	log IAP	log KT	
Al(OH) ₃ (a)	-2.16	8.97	11.13	Al(OH) ₃
Albite	-1.86	-20.19	-18.33	NaAlSi ₃ O ₈
Alunite	-7.18	-7.95	-0.77	KAl ₃ (SO ₄) ₂ (OH) ₆
Anhydrite	-3.63	-7.98	-4.34	CaSO ₄
Anorthite	-4.30	-24.16	-19.86	CaAl ₂ Si ₂ O ₈
Aragonite	-0.68	-8.98	-8.31	CaCO ₃
Ca-Montmorillonite	3.42	-42.34	-45.76	Ca _{0.165} Al _{2.33} Si _{3.67010} (OH) ₂
Calcite	-0.53	-8.98	-8.45	CaCO ₃
Celestite	-6.63	-13.25	-6.62	SrSO ₄
CH ₄ (g)	-132.33	-135.13	-2.80	CH ₄
Chalcedony	0.64	-2.97	-3.61	SiO ₂
Chlorite(14A)	-13.05	57.22	70.27	Mg ₅ Al ₂ Si ₃ O ₁₀ (OH) ₈
Chrysotile	-9.86	22.97	32.83	Mg ₃ Si ₂ O ₅ (OH) ₄

CO ₂ (g)	-1.04	-2.45	-1.41	CO ₂
Dolomite	-1.58	-18.55	-16.97	CaMg(CO ₃) ₂
Fe(OH) ₃ (a)	-0.38	4.51	4.89	Fe(OH) ₃
FeS(ppt)	-139.71	-143.62	-3.92	FeS
Gibbsite	0.58	8.97	8.40	Al(OH) ₃
Goethite	5.33	4.51	-0.82	FeOOH
Gypsum	-3.39	-7.98	-4.58	CaSO ₄ ·2H ₂ O
H ₂ (g)	-39.39	4.44	43.83	H ₂
H ₂ O(g)	-1.64	-0.00	1.64	H ₂ O
H ₂ S(g)	-133.55	-141.55	-8.00	H ₂ S
Halite	-9.77	-8.20	1.57	NaCl
Hausmannite	-7.77	54.52	62.29	Mn ₃ O ₄
Hematite	12.64	9.01	-3.62	Fe ₂ O ₃
Illite	1.18	-39.77	-40.95	K _{0.6} Mg _{0.25} Al _{2.3} Si _{3.5} O ₁₀ (OH) ₂
Jarosite-K	-12.52	-21.34	-8.82	KFe ₃ (SO ₄) ₂ (OH) ₆
K-feldspar	-0.63	-21.59	-20.96	KAlSi ₃ O ₈
K-mica	6.10	19.55	13.45	KAl ₃ Si ₃ O ₁₀ (OH) ₂
Kaolinite	4.13	12.01	7.88	Al ₂ Si ₂ O ₅ (OH) ₄
Mackinawite	-138.98	-143.62	-4.65	FeS
Manganite	-0.59	24.75	25.34	MnOOH
Melanterite	-18.00	-20.27	-2.27	FeSO ₄ ·7H ₂ O
N ₂ (g)	-5.49	-8.64	-3.14	N ₂
O ₂ (g)	-6.03	-8.89	-2.85	O ₂
Pyrite	-227.12	-245.74	-18.62	FeS ₂
Pyrochroite	-10.17	5.03	15.20	Mn(OH) ₂
Pyrolusite	2.27	44.47	42.19	MnO ₂ ·H ₂ O
Quartz	1.07	-2.97	-4.04	SiO ₂
Rhodochrosite	-3.07	-14.18	-11.11	MnCO ₃
Sepiolite	-5.52	10.37	15.89	Mg ₂ Si ₃ O _{7.5} OH·3H ₂ O
Sepiolite(d)	-8.29	10.37	18.66	Mg ₂ Si ₃ O _{7.5} OH·3H ₂ O
Siderite	-10.42	-21.28	-10.86	FeCO ₃
SiO ₂ (a)	-0.21	-2.97	-2.75	SiO ₂
Strontianite	-4.99	-14.26	-9.27	SrCO ₃
Sulfur	-100.10	-95.10	5.00	S
Talc	-4.94	17.04	21.98	Mg ₃ Si ₄ O ₁₀ (OH) ₂

 End of simulation.

Reading input data for simulation 2.

End of run.

No memory leaks

Scientific Research Publishing (SCIRP) is one of the largest Open Access journal publishers. It is currently publishing more than 200 open access, online, peer-reviewed journals covering a wide range of academic disciplines. SCIRP serves the worldwide academic communities and contributes to the progress and application of science with its publication.

Other selected journals from SCIRP are listed as below. Submit your manuscript to us via either submit@scirp.org or [Online Submission Portal](#).

